



FULL LENGTH ARTICLE

LKB1 depletion-mediated epithelial–mesenchymal transition induces fibroblast activation in lung fibrosis

Zijian Xu ^{a,1}, Elizabeth R. Davies ^{a,b,1}, Liudi Yao ^a, Yilu Zhou ^{a,c},
 Juanjuan Li ^a, Aiman Alzetani ^{d,e}, Ben G. Marshall ^{d,e},
 David Hancock ^f, Tim Wallis ^{d,e}, Julian Downward ^f,
 Rob M. Ewing ^{a,c}, Donna E. Davies ^{b,c,d}, Mark G. Jones ^{b,c,d,**},
 Yihua Wang ^{a,c,d,*}

^a Biological Sciences, Faculty of Environmental and Life Sciences, University of Southampton, Southampton SO17 1BJ, UK

^b Clinical and Experimental Sciences, Faculty of Medicine, University of Southampton, Southampton SO16 6YD, UK

^c Institute for Life Sciences, University of Southampton, Southampton SO17 1BJ, UK

^d NIHR Southampton Biomedical Research Centre, University Hospital Southampton, Southampton SO16 6YD, UK

^e University Hospital Southampton, Southampton SO16 6YD, UK

^f Oncogene Biology, The Francis Crick Institute, London NW1 1AT, UK

Received 7 February 2023; received in revised form 29 May 2023; accepted 28 June 2023

Available online 2 August 2023

KEYWORDS

LKB1;
 CAB39L;
 EMT;
 Crosstalk;
 Pulmonary fibrosis

Abstract The factors that determine fibrosis progression or normal tissue repair are largely unknown. We previously demonstrated that autophagy inhibition-mediated epithelial–mesenchymal transition (EMT) in human alveolar epithelial type II (ATII) cells augments local myofibroblast differentiation in pulmonary fibrosis by paracrine signaling. Here, we report that liver kinase B1 (LKB1) inactivation in ATII cells inhibits autophagy and induces EMT as a consequence. In IPF lungs, this is caused by the down-regulation of *CAB39L*, a key subunit within the LKB1 complex. 3D co-cultures of ATII cells and MRC5 lung fibroblasts coupled with RNA sequencing (RNA-seq) confirmed that paracrine signaling between LKB1-depleted ATII cells and fibroblasts augmented myofibroblast differentiation. Together, these data suggest that

* Corresponding author. Biological Sciences, Faculty of Environmental and Life Sciences, University of Southampton, Southampton SO17 1BJ, UK.

** Corresponding author. Clinical and Experimental Sciences, Faculty of Medicine, University of Southampton, Southampton SO16 6YD, UK. E-mail addresses: mark.jones@soton.ac.uk (M.G. Jones), yihua.wang@soton.ac.uk (Y. Wang).

Peer review under responsibility of Chongqing Medical University.

¹ These authors contributed equally to this work.

reduced autophagy caused by LKB1 inhibition can induce EMT in ATII cells and contribute to fibrosis via aberrant epithelial–fibroblast crosstalk.

© 2023 The Authors. Publishing services by Elsevier B.V. on behalf of KeAi Communications Co., Ltd. This is an open access article under the CC BY license (<http://creativecommons.org/licenses/by/4.0/>).

Introduction

Idiopathic pulmonary fibrosis (IPF) is a chronic, progressive, fibrotic lung disease of unknown etiology.¹ In IPF the current paradigm of disease pathogenesis proposes that the delicate alveolar architecture of the lung is disrupted by extracellular matrix (ECM) deposition as a consequence of repetitive micro-injuries to the alveolar epithelium, resulting in tissue scarring, increased stiffness, and impaired gas exchange. Two anti-fibrotic drugs, nintedanib and pirfenidone, are approved worldwide for the treatment of IPF however whilst there is evidence that they can slow disease progression they cannot stop or reverse it² and so better treatments are urgently required.

We previously identified that alveolar epithelial type II (ATII) cells undergoing epithelial–mesenchymal transition (EMT) promote a pro-fibrotic microenvironment through paracrine signaling activating local fibroblasts.^{3–5} EMT is a dynamic, reversible process that has been implicated in embryonic development, wound healing, cancer metastasis, and fibrosis.⁶ Induction of EMT in fibrosis has been linked to a variety of processes including autophagy inhibition which triggers EMT via the p62/SQSM1-NFκB-Snail2 signaling pathway.^{3,7} Autophagy (macro-autophagy) is a regulated self-management mechanism allowing the bulk or selective degradation of intracellular components and has been widely associated with several aging processes including neurodegeneration, cancer, and fibrosis.⁸ It has been reported that autophagy activity is reduced in IPF,^{9–13} however, signaling pathways leading to this phenomenon remain to be elucidated. Here, we report that the inactivation of liver kinase B1 (LKB1, encoded by the gene *Serine/Threonine Kinase 11*, *STK11*) in ATII cells inhibits autophagy and induces EMT. We identified down-regulation of *CAB39L*, the allosteric activator of LKB1 in IPF alveolar septae, and found that levels of *CAB39L* were significantly inversely correlated with *SNAI2* (Snail2) suggesting that reduction of *CAB39L* in IPF alveolar epithelium leads to LKB1 inactivation and promotes EMT. The profibrotic relevance of alveolar LKB1 inactivation was demonstrated in 3D co-cultures of ATII cells and lung fibroblasts in which paracrine signaling between LKB1-depleted ATII cells and fibroblasts was shown to augment myofibroblast differentiation.

Materials and methods

Cell culture, reagents, and transfections

Sources of cell lines, culture conditions, and short interfering RNA (siRNA) transfections were reported earlier.^{3–5,14–17} MRC5 lung fibroblasts were obtained from the

European Collection of Authenticated Cell Cultures (ECACC). Fibroblasts were cultured in Dulbecco's Modified Eagle's Medium (DMEM) supplemented with 10% fetal bovine serum (FBS), 50 units/mL penicillin, 50 µg/mL streptomycin, 2 mM l-glutamine, 1 mM sodium pyruvate, and 1× non-essential amino acids (all from Life Technologies). An alveolar type II (ATII) cell line^{18,19,5} was cultured in DCCM-1 (Biological Industries Ltd) supplemented with 10% new-born calf serum (NBCS) (Life Technologies), 1% penicillin, 1% streptomycin, and 1% l-glutamine (all from Life Technologies). The human ATII cell line grows in continuous culture and expresses the ATII cell marker, pro-surfactant protein C (ProSP-C).^{3,5} All cells were kept at 37 °C and 5% CO₂. All cultures were tested and free of mycoplasma contamination. Details are provided in the [Supplementary methods](#).

Three-dimensional (3D) co-cultures

Aggregation of 3D co-cultures was achieved using Nanoshuttle-PL (Greiner Bio-One). Briefly, MRC5 fibroblasts at 80% confluence were treated with Nanoshuttle-PL for 24 h, before trypsinization. Cells were then pipetted onto cell-repellant 96-well plates sat on a magnetic drive and left to incubate at 37 °C and 5% CO₂ for a minimum of 3 h on the magnetic drive to enable the spheroid to form. The process was then repeated for control or LKB1-depleted ATII cells so they could then grow around the existing fibroblast spheroid. LKB1-depleted ATII cells were generated by transfection with LKB1 (*STK11*) siRNA oligos at a final concentration of 35 nM using DharmaFECT 2 reagent (Dharmacon).

Lung tissue sampling

All human lung tissue samples for primary cell culture were approved by the Southampton and South West Hampshire and the Mid and South Buckinghamshire Local Research Ethics Committees, and all subjects gave written informed consent. Clinically indicated IPF lung biopsy tissue samples and non-fibrotic control tissue samples (macroscopically normal lung sampled remote from a cancer site) were assessed as surplus to clinical diagnostic requirements. All IPF samples were from patients subsequently receiving a multidisciplinary diagnosis of IPF according to international consensus guidelines.²⁰

RNA *in situ* hybridization

In situ detection of *CAB39L* mRNA on formalin-fixed paraffin-embedded (FFPE) sections of lung tissue from patients with IPF or non-fibrotic control was performed using RNAscope® technology (Advanced Cell Diagnostics, Biotechne,

Abingdon, UK) ($n = 3$ samples each group).¹⁵ *CAB39L* mRNA was detected by the predesigned probe. Briefly, lung tissue sections (thicknesses: 5 μm) were baked at 60 $^{\circ}\text{C}$, deparaffinized in xylene, followed by dehydration in graded ethanol. Target retrieval, hybridization with target probe, amplification, and chromogenic detection were performed according to the manufacturer's recommendations (RNAscope 2.5 HD Assay-RED for FFPE tissues). Sections were counterstained with Gill's hematoxylin and mounted with Vectamount prior to imaging. Assays were performed with positive (peptidylprolyl isomerase B, *PPIB*) and negative controls. Images were acquired using an Olympus Scanner VS110 (Olympus UK, Southend-on-Sea, UK).

Methods for RNA-seq and bioinformatics, Western blot, real-time qPCR; immunofluorescence microscopy, and luciferase reporter assay and statistical analysis

were reported earlier,^{3–5,14–17} with details provided in the [Supplementary methods](#).

Results

Global transcriptomic changes in LKB1-depleted alveolar type II (ATII) cells

It was reported previously that activation of AMP-activated protein kinase (AMPK), a downstream effector of LKB1, in myofibroblasts from IPF lungs reduces fibrogenic activity.²¹ To determine if, and how, ATII cells responded to alteration of LKB1 activity, we characterized the global transcriptomic changes in ATII cells upon RNA interference (RNAi)-mediated LKB1 depletion by performing RNA-seq. The human ATII cell line grows in continuous culture and expresses the ATII cell marker, pro-surfactant protein C, as reported earlier.⁷

Differentially expressed genes (DEGs) were defined by a false discovery rate (FDR)-adjusted P value (P_{adj}) less than 0.05 and $|\text{Log}_2\text{Fold Change}|$ above 1. In total, 763 up-regulated and 664 down-regulated DEGs were identified (Table S1). Gene Ontology (GO) enrichment analysis was performed and grouped into molecular function, biological process, and cellular component. Of note, several EMT-related terms were identified, including cell junction, chemotaxis, and regulation of cell migration (FDR < 0.05; Fig. 1A; Fig. S1 and Table S2). To provide further mechanistic insights, Gene Set Enrichment Analysis (GSEA)²² was performed and several Hallmark pathways were identified, including "TNF α signaling pathway via NF κ B" and "EMT" as the top up-regulated pathways in LKB1-depleted ATII cells (Fig. 1B and Table S3).

LKB1 depletion in ATII cells induces EMT

Given that the "Hallmark_EMT" pathway was positively enriched upon LKB1 (*STK11*) depletion in ATII cells (Fig. 2A; normalized enrichment score, NES = 2.03; FDR < 0.001), we examined changes in EMT-associated genes. We identified increases in expression of *VIM* (Vimentin, a

mesenchymal marker) and several EMT-transcriptional factors, in particular, *SNAIL2* (encoding Snail2), as well as a reduction in *CDH1* (encoding E-cadherin, an epithelial marker) in our RNA-seq dataset (Fig. 2B) which we confirmed by real-time qPCR (Fig. 2C), as well as demonstrating increased protein levels of Snail2 while E-cadherin protein was decreased (Fig. 2D). Together, these results demonstrate that loss of LKB1 activates an EMT program in ATII cells.

LKB1 depletion leads to autophagy inhibition-mediated EMT via the p62-NF κ B-Snail2 pathway in ATII cells

Another highly enriched pathway in LKB1-depleted ATII cells was "Hallmark_TNF α signaling pathway via NF κ B" (Fig. S2A; normalized enrichment score, NES = 2.45; FDR < 0.001). To verify this, we assessed NF κ B activity using a reporter assay identifying that LKB1 depletion in ATII cells increased NF κ B activity above 2-fold (Fig. S2B; $P < 0.01$).

We have previously demonstrated that autophagy inhibition induced accumulation of p62/*SQSM1* and activation of the NF κ B pathway.^{3,16} Given our identification of increased NF κ B activity upon LKB1 silencing, we, therefore, investigated the role of LKB1 on autophagy activity in ATII cells. This identified that LKB1 depletion in ATII cells led to autophagy inhibition, as demonstrated by decreased levels of LC3-II and increased p62 by Western blot analysis (Fig. 3A), as well as punctate staining for p62 by immunofluorescence (Fig. 3B).

We next checked if LKB1 depletion induced EMT via the p62-NF κ B-Snail2 pathway. Depletion of p62 abolished the increase in NF κ B activity induced by LKB1 knockdown (Fig. 3C), suggesting that LKB1 depletion in ATII cells triggers the NF κ B pathway via p62. Functionally, the knockdown of either NF κ B p65 (Fig. 3D) or p62 (Fig. 3E) abolished the increase in Snail2 expression induced by LKB1 depletion in ATII cells. Taken together, these results demonstrate that LKB1 inactivation in ATII cells inhibits autophagy and promotes EMT via a p62-NF κ B pathway.

Down-regulation of *CAB39L* in human IPF lungs

Activation of LKB1 occurs via allosteric binding of LKB1 to STE20-related adapter (*STRAD*) and mouse protein 25 (MO25, encoded by *CAB39* and *CAB39L*).²³ Given our *in vitro* findings, we compared the expression of LKB1 (*STK11*), *STRADA*, *STRADB*, *CAB39*, and *CAB39L* in IPF and control lungs in a transcriptomic dataset that we have recently established (GSE169500).¹⁵ Briefly, laser capture microdissection was performed upon formalin-fixed paraffin-embedded (FFPE) control non-fibrotic lung tissue (alveolar septae, $n = 10$) and usual interstitial pneumonia/idiopathic pulmonary fibrosis FFPE lung tissue (fibroblast foci and adjacent non-affected alveolar septae, $n = 10$ each), followed by RNA-seq. Among those subunits within the LKB1 complex, only the expression of *CAB39L*, the allosteric activator of LKB1, was down-regulated in IPF alveolar septae (Fig. 4A). By contrast, the expression of other subunits, including LKB1 (*STK11*), *STRADA*, *STRADB*, and *CAB39*, did

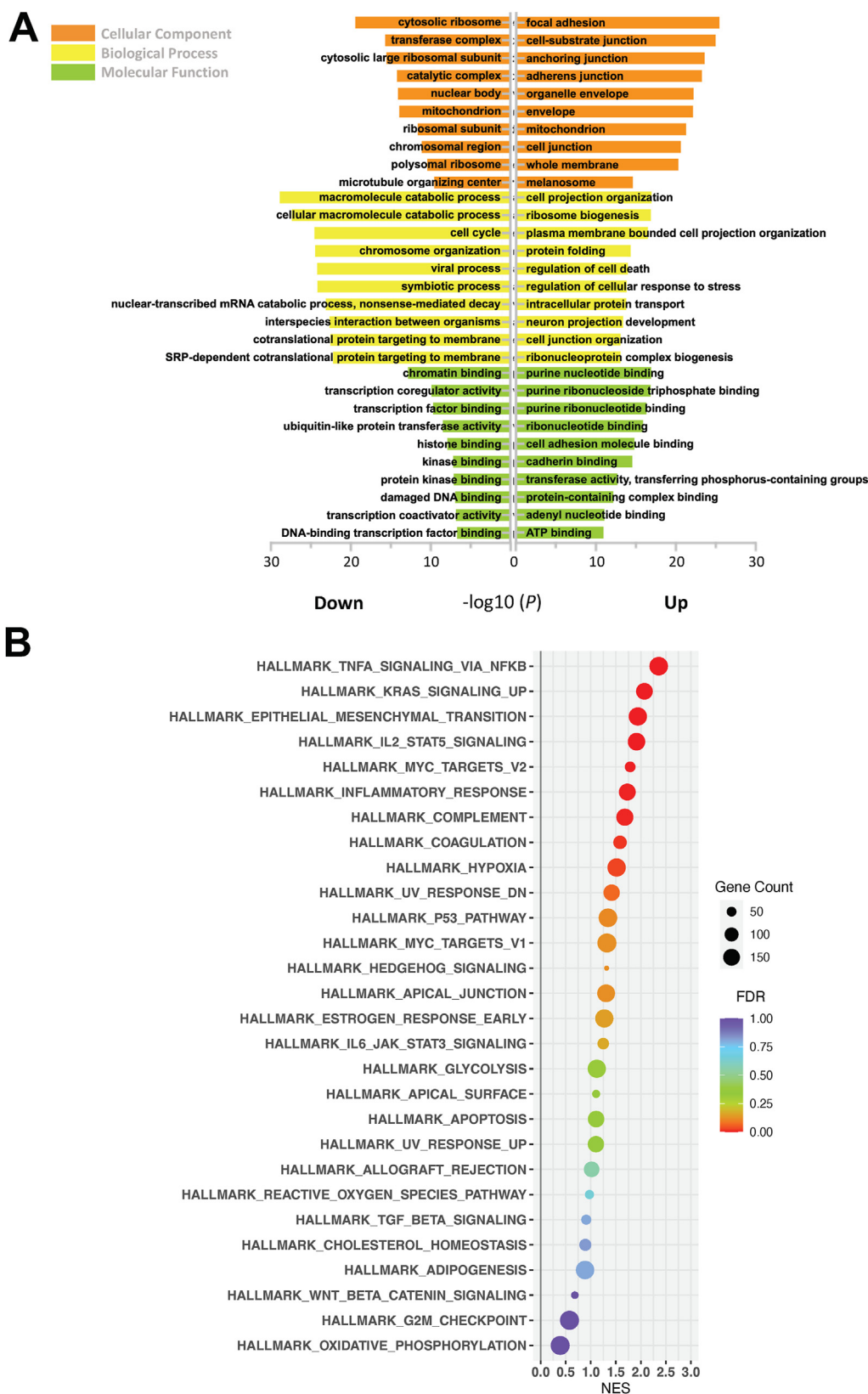


Figure 1 Global transcriptomic changes in LKB1-depleted A11 cells. **(A)** The bar plot showing Gene Ontology (GO) enrichment of up-regulated and down-regulated differentially expressed genes (DEGs) in three groups: cellular component (orange), biological processes (yellow), and molecular functions (green). The top 10 enriched GO terms are arranged in $-\log_{10}(P)$ -value. **(B)** The scatter plot showing Gene Set Enrichment Analysis (GSEA). Results are ranked by the normalized enrichment score (NES). The color and size of the dots represent the false discovery rate (FDR) and gene counts, respectively.

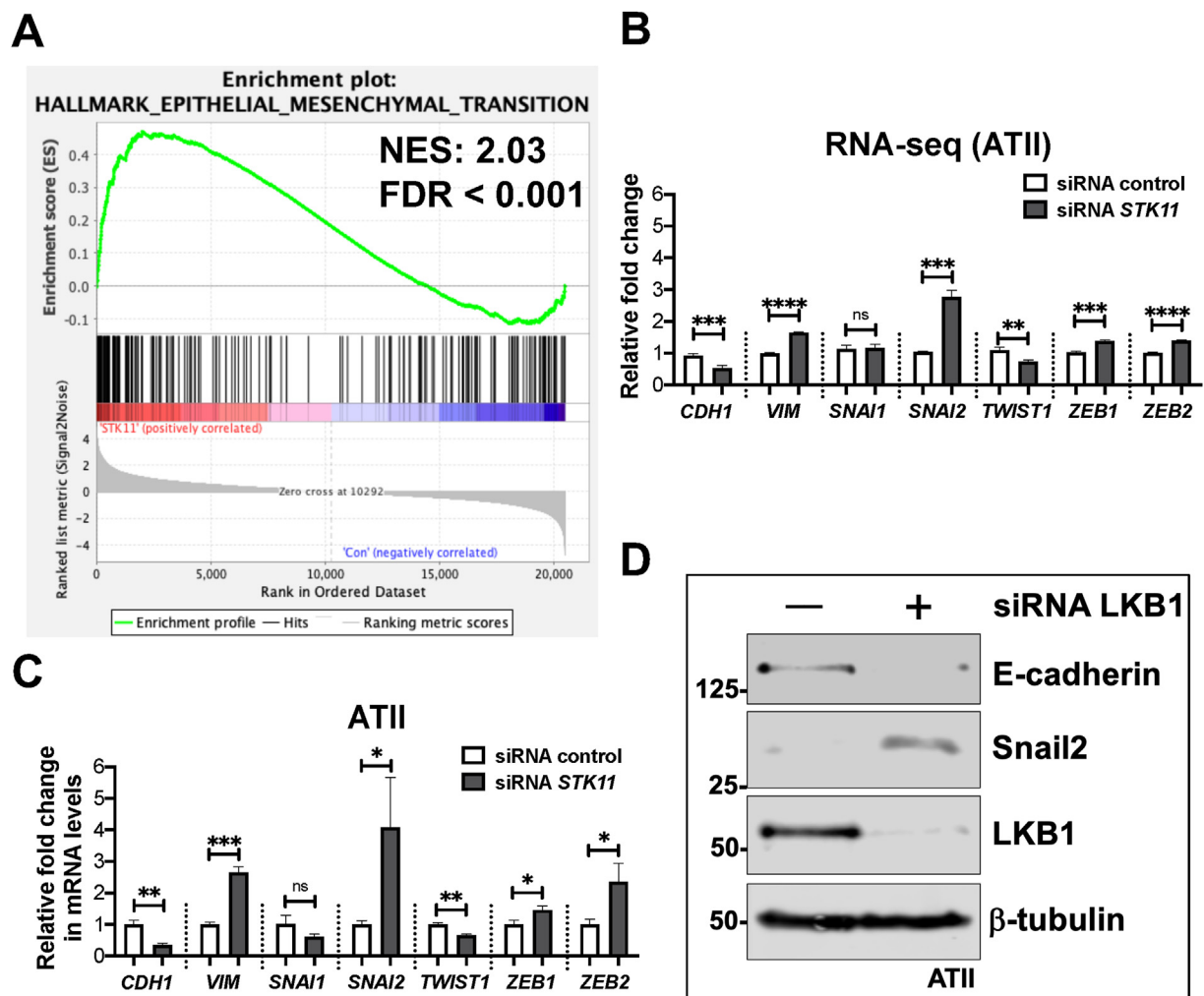


Figure 2 LKB1 depletion in ATII cells induces EMT. (A) The Gene Set Enrichment Analysis (GSEA) plot showing the enrichment of Hallmark_Epithelial–Mesenchymal Transition in LKB1-depleted ATII cells. Normalized enrichment score (NES) and false discovery rate (FDR) are indicated. (B) The RNA-seq data showing relative expressions of *CDH1* (encoding E-cadherin), *VIM* (encoding Vimentin), *SNAI1* (encoding Snail1), *SNAI2* (encoding Snail2), *TWIST1*, *ZEB1*, and *ZEB2* in LKB1-depleted ATII cells versus control. The data were expressed as mean \pm standard deviation. $n = 3$ samples in each group; ** $P < 0.01$, *** $P < 0.001$, **** $P < 0.0001$; ns, not significant. (C) Relative fold changes in mRNA levels of *CDH1* (E-cadherin), *VIM* (Vimentin), *SNAI1* (Snail1), *SNAI2* (Snail2), *TWIST1*, *ZEB1*, and *ZEB2* in LKB1-depleted ATII cells versus control. *ACTB* (encoding β -actin)-normalized mRNA levels in ATII cells were used to set the baseline value at unity. The data were expressed as mean \pm standard deviation. $n = 3$ samples in each group; * $P < 0.05$, ** $P < 0.01$, *** $P < 0.001$; ns, not significant. (D) Protein expressions of E-cadherin, Snail2, and LKB1 in ATII cells transfected with the indicated siRNA. β -Tubulin was used as a loading control.

not significantly change in IPF lungs (Fig. S3). Down-regulation of *CAB39L* in human IPF lung tissue was confirmed using real-time qPCR of IPF lung tissue lysates (Fig. 4B; $P < 0.05$) as well as RNA *in situ* hybridization of alveolar septae (Fig. 4C). We also assessed the expression of *CAB39L* and *SNAI2* (encoding Snail2) in alveolar septae from control and IPF lungs using the same dataset (GSE169500) and found that the levels of *CAB39L* were significantly inversely correlated with *SNAI2* (Snail2) (Fig. 4D; Pearson $r = -0.65$; $n = 20$; $P = 0.002$). These observations support the concept that in IPF alveolar epithelium down-regulation of *CAB39L* leads to LKB1 inactivation and promotes EMT via the p62-NF κ B pathway (Fig. 4E).

3D co-cultures of ATII cells and pulmonary fibroblasts suggest the involvement of paracrine signaling in augmenting myofibroblast differentiation

Our previous study reported that reduced autophagy activity contributed to fibrosis via aberrant epithelial-fibroblast crosstalk.³ To determine if it was also the case for LKB1-depletion in ATII cells, 2D cultures of ATII cells alone or 3D co-cultures with MRC5 lung fibroblasts (Fig. 5A) were established and then analyzed by RNA-seq. DEGs were defined by an FDR-adjusted P value (P_{adj}) less than 0.05 and $|\text{Log}_2\text{Fold Change}|$ above 1 (Table S4).

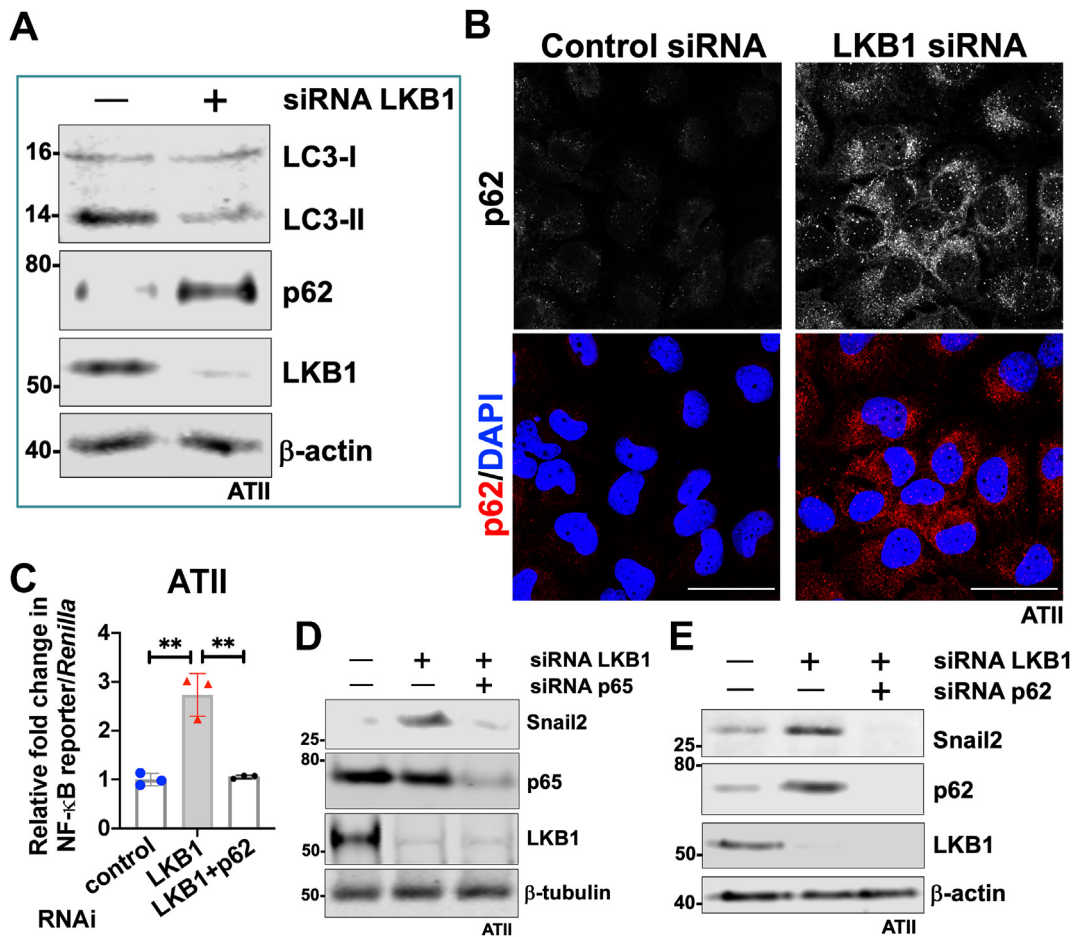


Figure 3 LKB1 depletion leads to autophagy inhibition-mediated EMT via the p62-NFκB-Snail2 pathway in ATII cells. **(A)** Protein expression of LC3-I, LC3-II, p62, and LKB1 in ATII cells transfected with the indicated siRNA. β-actin was used as a loading control. **(B)** Immunofluorescence staining of p62 (red) in ATII cells transfected with the indicated siRNA. DAPI (blue) was used to stain nuclei. Scale bar, 40 μm. **(C)** NF-κB reporter assays in ATII cells with the indicated treatment. Values represent the relative fold of *Renilla* luciferase, normalized against control (1.0). The data were expressed as mean ± standard deviation. $n = 3$ samples in each group; $**P < 0.01$. **(D)** Protein expression of Snail2, p65, and LKB1 in ATII cells with the indicated treatment. β-Tubulin was used as a loading control. **(E)** Protein expression of Snail2, p62, and LKB1 in ATII cells with the indicated treatment. β-actin was used as a loading control.

Our earlier reports^{3,5} by comparison of the relative expression of ECM components in ATII cells and fibroblasts highlight that ATII cells produce extremely low levels of ECM genes even after the induction of EMT, suggesting that ECM production in fibrosis is more likely to be a consequence of fibroblast activation than direct deposition by epithelial cells undergoing EMT. This is also true in this study. A comparison of collagen genes in 2D monocultures of control or LKB1-depleted ATII showed relatively low levels of collagen gene expression that were not significantly different (control ATII vs. LKB1-depleted ATII; Fig. 5B and Table S5), even though an EMT signature was clearly detectable in the LKB1 depleted cells (Fig. 1, 2). In contrast, when LKB1-depleted ATII cells were co-cultured with MRC5 fibroblasts, there was a marked up-regulation of a large number of collagen genes (control ATII + MRC5 vs. LKB1-depleted ATII + MRC5; Fig. 5B and Table S5). Quantification of the changes in collagen gene expression

using gene set variation analysis (GSVA),²⁴ identified a significant effect of LKB1 depletion in 3D co-cultures of ATII cells and MRC5 (Fig. 5C; $P < 0.01$), but not in 2D-cultured ATII cells (Fig. 5C; $P > 0.05$). This suggested collagen production in IPF lungs is unlikely to be a direct consequence of epithelial collagen gene expression due to EMT, but rather epithelial cells exhibiting an indirect effect on fibroblast differentiation via paracrine signaling, especially when undergoing EMT.^{3,5}

To further explore the effect of paracrine signaling on fibroblast to myofibroblast transition, in 3D co-cultures we analyzed the expression of *ACTA2* (α-SMA, a myofibroblast marker), confirming that LKB1 depletion in ATII cells caused increased expression and that this was associated with up-regulation in *COL1A1*, *COL3A1*, and *FN1* (Fig. 5D; all $P < 0.01$). Finally, to confirm the paracrine influence of ATII cells on fibroblast differentiation, we treated MRC5 cells with conditioned media (CM) from ATII cells transfected

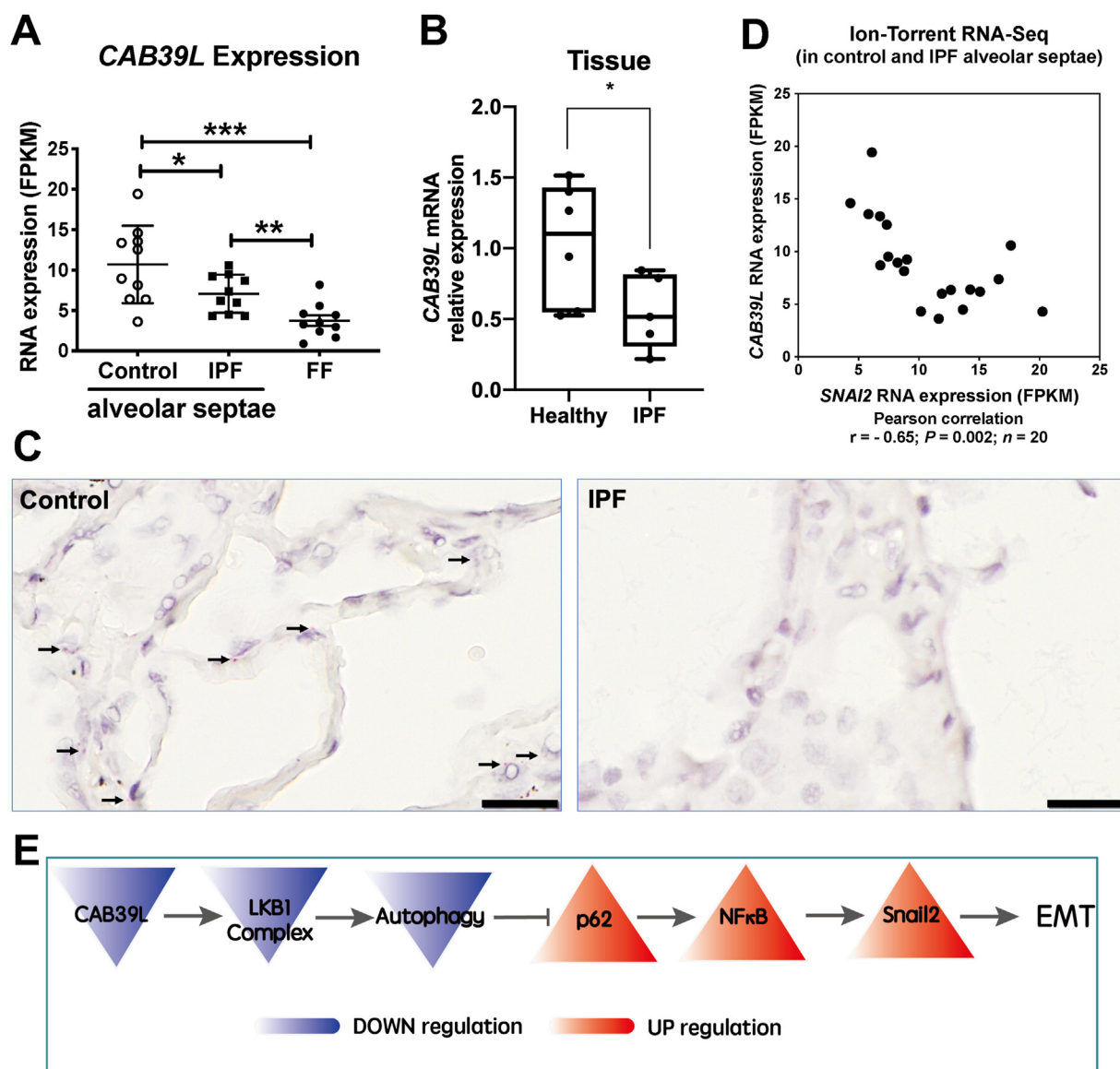


Figure 4 Down-regulation of *CAB39L* in human IPF lungs. (A) Expression of *CAB39L* in healthy (control) alveolar septae, IPF alveolar septae, and IPF fibroblast foci ($n = 10$ individual healthy and IPF donors; GSE169500). Relative expression levels are calculated as Fragments Per Kilobase of transcript per Million mapped reads (FPKM). The data were expressed as mean \pm standard deviation. $n = 10$ samples in each group; $*P < 0.05$, $**P < 0.01$, $***P < 0.001$. (B) Relative fold changes in the mRNA level of *CAB39L* in human non-fibrotic control versus IPF lung tissue. The data were expressed as mean \pm standard deviation. $n = 6$ samples in each group; $*P < 0.05$. (C) Representative images of mRNA expression of *CAB39L* (arrows) in non-fibrotic control or IPF lung tissue using RNAscope® RNA *in situ* hybridization. Scale bar, 20 μ m. (D) The scatter plot for comparing the expression of *CAB39L* and *SNAI2* (Snail2) in alveolar septae from non-fibrotic control and IPF lung tissue (Pearson coefficient $r = -0.65$; $P = 0.002$; $n = 20$). (E) The diagram showing that *CAB39L* down-regulation in IPF inactivates LKB1 complex, leading to autophagy inhibition-mediated EMT via the p62-NF κ B-Snail2 pathway in ATII cells.

with control or LKB1 siRNA without or with the addition of transforming growth factor- β (TGF- β), and assessed levels of α -SMA. CM from ATII cells transfected with LKB1 siRNA without TGF- β had a similar effect on α -SMA expression compared with TGF- β treatment alone (Fig. 5E). Furthermore, CM from LKB1-depleted ATII cells together with TGF- β achieved a strong synergistic effect on α -SMA protein levels (Fig. 5E). These data suggest that LKB1 depletion in ATII cells augments myofibroblast differentiation via paracrine signaling.

Discussion

IPF is a progressive interstitial lung disease with limited treatment options available.²⁵ Although the underlying cause of IPF is not fully understood, repetitive micro-injuries to aged alveolar epithelium are proposed to trigger aberrant wound healing processes, initiating an accumulation of ECM deposited by myofibroblasts,²⁶ which are critical in the pathogenesis of IPF, with increased fibroblast

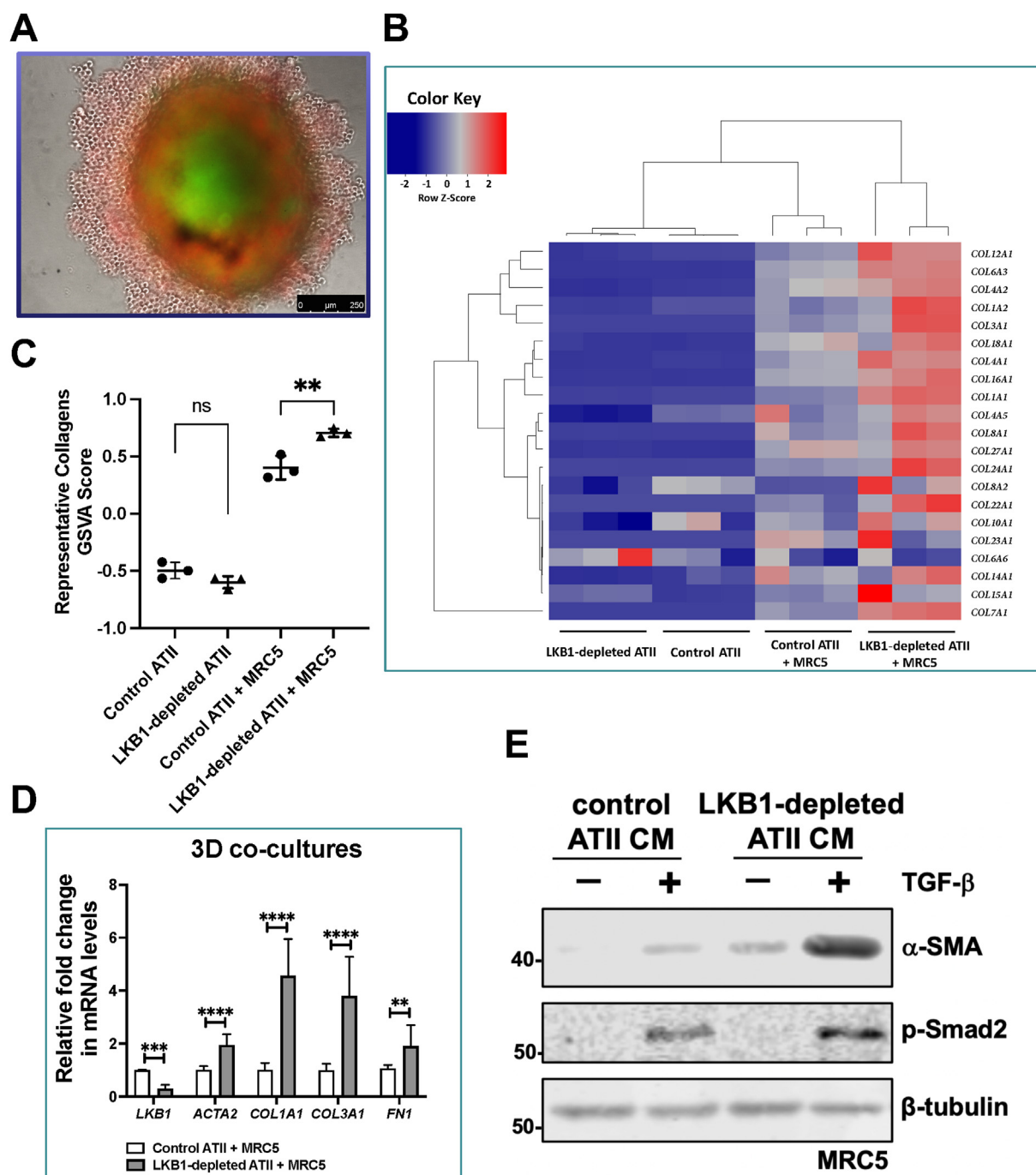


Figure 5 3D co-cultures of ATII cells and MRC5 coupled with RNA-seq suggest a role of paracrine signaling in augmenting myofibroblast differentiation. **(A)** A representative image showing a 3D co-culture spheroid of MRC5 lung fibroblasts (green) and ATII cells (red). Scale bar, 250 μ m. **(B)** Heatmap and hierarchical cluster analysis of multiple collagen genes in 2D-cultured control or LKB1-depleted ATII cells and 3D co-cultures of MRC5 with control or LKB1-depleted ATII cells. The red indicates up-regulation and the blue down-regulation. $n = 3$ samples in each group. **(C)** The graph showing Gene Set Variation Analysis (GSEA) scores using a collagen signature in 2D-cultured control or LKB1-depleted ATII cells, and 3D co-cultures of MRC5 with control or LKB1-depleted ATII cells. The data were expressed as mean \pm standard deviation. $n = 3$ samples in each group; $**P < 0.01$; ns, not significant. **(D)** Relative mRNA expression of *STK11* (encoding LKB1), *ACTA2* (encoding α -SMA), *COL1A1*, *COL3A1*, and *FN1* in the spheroid samples from MRC5 co-cultured with control or LKB1-depleted ATII cells. *ACTB* (encoding β -actin)-normalized mRNA levels in ATII cells were used to set the baseline value at unity. The data were expressed as mean \pm standard deviation. $n = 3$ samples in each group; $**P < 0.01$, $***P < 0.001$, $****P < 0.0001$. **(E)** Protein expression of α -SMA and phospho-Smad2 (p-Smad2) in MRC5 with indicated treatments. β -Tubulin was used as a loading control.

foci associated with worse prognosis.²⁷ The origin of myofibroblasts in IPF is controversial and it was proposed that ATII cells undergoing EMT may be a source of myofibroblasts in fibrotic diseases. However, findings from our group suggest that ATII cells undergoing EMT induced by RAS activation⁵ or autophagy inhibition³ express only low levels of ECM genes. Our findings in this study support the concept that epithelial cells do not directly contribute to myofibroblast populations via EMT, instead, they are able to promote myofibroblast differentiation through paracrine signaling.⁷

LKB1 is an evolutionarily conserved serine/threonine protein kinase, which acts as an important regulator of cell polarity, proliferation, and cell metabolism in epithelial cells.²⁸ Activation of LKB1 occurs via allosteric binding of LKB1 to STE20-related adapter (*STRAD*) and mouse protein 25 (MO25, encoded by *CAB39* and *CAB39L*).²⁹ Many of the best-known functions of LKB1 are attributable to its ability to activate AMPK, which is an important conserved regulator of cell growth and metabolism.³⁰ It was reported recently that activation of AMPK in myofibroblasts from IPF lungs displays lower fibrotic activity. In a bleomycin mouse model of lung fibrosis, metformin accelerates the resolution of well-established fibrosis in an AMPK-dependent manner.²¹ This study supports a role for such an approach to reverse established fibrosis by facilitating the deactivation and apoptosis of myofibroblasts.²¹ In line with this, a recent study suggests that in patients with IPF and type 2 diabetes, metformin therapy may be associated with improved clinical outcomes. However, further investigation with randomized clinical trials is necessary prior to metformin's broad implementation in the clinical management of IPF.³¹

Han and colleagues reported that kidney-specific deletion of *Lkb1* induces severe renal fibrosis.³² Similar to our findings, they found LKB1 (*STK11*) mRNA levels are not significantly altered in fibrotic kidney samples. Instead, the expression of the allosteric activator of LKB1, *CAB39L*, significantly decreases in kidney fibrosis,³² raising its potential role in the development of fibrotic disease. Coincidentally, thymoquinone alleviates thioacetamide-induced hepatic fibrosis by activating the LKB1-AMPK signaling pathway in mice.³³ Apart from AMPK, LKB1 also activates a family of 12 "AMPK-related kinases", including BRSK1, BRSK2, NUA1, NUA2, QIK, QSK, SIK, MARK1, MARK2, MARK3, MARK4, and MELK.³⁴ It was shown earlier that LKB1 suppresses EMT-transcriptional factor Snail1³⁵ and ZEB1³⁶ expression via MARK1/4 and miR-200a/c, respectively. In this study, we demonstrated that LKB1 depletion induces Snail2 expression via autophagy inhibition-p62-NF κ B pathway in ATII cells, consistent with our previous reports.^{3,16}

As a highly conserved process,³⁷ autophagy has been associated with several human diseases, including pulmonary fibrosis (see our recent review³⁸). It has been reported that LKB1 modulates autophagy activity via an AMPK-mTORC1^{39,40} or AMPK-ULK1 (ATG1) axis.⁴¹ In ATII cells, upon LKB1 inhibition, autophagy activity is reduced, leading to EMT via the p62-NF κ B pathway (Fig. 4E). This drives local myofibroblast differentiation via paracrine signaling.

In summary, this study provides novel insights into the role of epithelial LKB1 in pulmonary fibrosis, highlighting

the potential therapeutic intervention by targeting this pathway in IPF.

Conflict of interests

YW is an editorial board member for *Genes & Diseases* and was not involved in the editorial review or the decision to publish this article. All authors declare that there are no competing interests.

Funding

This project was supported by the UK Medical Research Council (MR/S025480/1), the UK Academy of Medical Sciences/the Wellcome Trust Springboard Award (SBF002\1038), and AAIR Charity. ZX and LY were supported by China Scholarship Council. YZ was supported by an Institute for Life Sciences PhD Studentship. JD was supported by the Francis Crick Institute which receives its core funding from Cancer Research UK (FC001070), the UK Medical Research Council (FC001070), and the Wellcome Trust (FC001070).

Data availability

All data generated or analyzed during this study are included in the manuscript and supporting files. The RNA-seq data have been deposited in the Gene Expression Omnibus (GEO) database (accession code GSE205970).

Acknowledgements

We thank Carine Fixmer, Maria Lane, Benjamin Johnson, and the nurses of the Southampton Biomedical Research Unit for their help in the collection of human samples, supported by the Wessex Clinical Research Network and the National Institute of Health Research, UK. The authors gratefully acknowledge the Imaging and Microscopy Centre at the Biological Sciences (The University of Southampton) for their support and assistance in this work. For the purpose of open access, the authors have applied a CC-BY public copyright license to any Author Accepted Manuscript version arising from this submission.

Appendix A. Supplementary data

Supplementary data to this article can be found online at <https://doi.org/10.1016/j.gendis.2023.06.034>.

References

1. Velagacherla V, Mehta CH, Nayak Y, Nayak UY. Molecular pathways and role of epigenetics in idiopathic pulmonary fibrosis. *Life Sci.* 2022;291:120283.
2. Raghu G, Selman M. Nintedanib and pirfenidone. New anti-fibrotic treatments indicated for idiopathic pulmonary fibrosis offer hopes and raises questions. *Am J Respir Crit Care Med.* 2015;191(3):252–254.

3. Hill C, Li J, Liu D, et al. Autophagy inhibition-mediated epithelial-mesenchymal transition augments local myofibroblast differentiation in pulmonary fibrosis. *Cell Death Dis.* 2019;10:591.
4. Yao L, Zhou Y, Li J, et al. Bidirectional epithelial-mesenchymal crosstalk provides self-sustaining profibrotic signals in pulmonary fibrosis. *J Biol Chem.* 2021;297(3):101096.
5. Yao L, Conforti F, Hill C, et al. Paracrine signalling during ZEB1-mediated epithelial-mesenchymal transition augments local myofibroblast differentiation in lung fibrosis. *Cell Death Differ.* 2019;26(5):943–957.
6. Jolly MK, Celià-Terrassa T. Dynamics of phenotypic heterogeneity associated with EMT and stemness during cancer progression. *J Clin Med.* 2019;8(10):1542.
7. Hill C, Jones MG, Davies DE, Wang Y. Epithelial-mesenchymal transition contributes to pulmonary fibrosis via aberrant epithelial/fibroblastic cross-talk. *J Lung Health Dis.* 2019;3(2):31–35.
8. Martinez-Lopez N, Athonvarangkul D, Singh R. Autophagy and aging. *Adv Exp Med Biol.* 2015;847:73–87.
9. Araya J, Kojima J, Takasaka N, et al. Insufficient autophagy in idiopathic pulmonary fibrosis. *Am J Physiol Lung Cell Mol Physiol.* 2013;304(1):L56–L69.
10. Patel AS, Lin L, Geyer A, et al. Autophagy in idiopathic pulmonary fibrosis. *PLoS One.* 2012;7(7):e41394.
11. Wang K, Zhang T, Lei Y, et al. Identification of ANXA2 (annexin A2) as a specific bleomycin target to induce pulmonary fibrosis by impeding TFEB-mediated autophagic flux. *Autophagy.* 2018;14(2):269–282.
12. Ricci A, Cherubini E, Scozzi D, et al. Decreased expression of autophagic beclin 1 protein in idiopathic pulmonary fibrosis fibroblasts. *J Cell Physiol.* 2013;228(7):1516–1524.
13. Cabrera S, Maciel M, Herrera I, et al. Essential role for the ATG4B protease and autophagy in bleomycin-induced pulmonary fibrosis. *Autophagy.* 2015;11(4):670–684.
14. Zhou Y, Hill C, Yao L, et al. Quantitative proteomic analysis in alveolar type II cells reveals the different capacities of RAS and TGF- β to induce epithelial–mesenchymal transition. *Front Mol Biosci.* 2021;8:595712.
15. Brereton CJ, Yao L, Davies ER, et al. Pseudohypoxic HIF pathway activation dysregulates collagen structure-function in human lung fibrosis. *Elife.* 2022;11:e69348.
16. Wang Y, Xiong H, Liu D, et al. Autophagy inhibition specifically promotes epithelial-mesenchymal transition and invasion in RAS-mutated cancer cells. *Autophagy.* 2019;15(5):886–899.
17. Wang Y, Bu F, Royer C, et al. ASPP2 controls epithelial plasticity and inhibits metastasis through β -catenin-dependent regulation of ZEB1. *Nat Cell Biol.* 2014;16(11):1092–1104.
18. Coelho MA, de Carné Trécesson S, Rana S, et al. Oncogenic RAS signaling promotes tumor immunoresistance by stabilizing PD-L1 mRNA. *Immunity.* 2017;47(6):1083–1099.e6.
19. Molina-Arcas M, Hancock DC, Sheridan C, Kumar MS, Downward J. Coordinate direct input of both KRAS and IGF1 receptor to activation of PI3 kinase in KRAS-mutant lung cancer. *Cancer Discov.* 2013;3(5):548–563.
20. Raghu G, Remy-Jardin M, Myers JL, et al. Diagnosis of idiopathic pulmonary fibrosis. An official ATS/ERS/JRS/ALAT clinical practice guideline. *Am J Respir Crit Care Med.* 2018;198(5):e44–e68.
21. Rangarajan S, Bone NB, Zmijewska AA, et al. Metformin reverses established lung fibrosis in a bleomycin model. *Nat Med.* 2018;24(8):1121–1127.
22. Subramanian A, Tamayo P, Mootha VK, et al. Gene set enrichment analysis: a knowledge-based approach for interpreting genome-wide expression profiles. *Proc Natl Acad Sci U S A.* 2005;102(43):15545–15550.
23. Zeqiraj E, Filippi BM, Deak M, Alessi DR, van Aalten DM. Structure of the LKB1-STRAD-MO25 complex reveals an allosteric mechanism of kinase activation. *Science.* 2009;326(5960):1707–1711.
24. Hänzelmann S, Castelo R, Guinney J. GSEA: gene set variation analysis for microarray and RNA-seq data. *BMC Bioinf.* 2013;14:7.
25. Richeldi L, Collard HR, Jones MG. Idiopathic pulmonary fibrosis. *Lancet.* 2017;389(10082):1941–1952.
26. Moss BJ, Ryter SW, Rosas IO. Pathogenic mechanisms underlying idiopathic pulmonary fibrosis. *Annu Rev Pathol Mech Dis.* 2022;17:515–546.
27. King TJR, Schwarz M, Brown K, et al. Idiopathic pulmonary fibrosis. *Am J Respir Crit Care Med.* 2001;164(6):1025–1032.
28. Kullmann L, Krahn MP. Controlling the master – upstream regulation of the tumor suppressor LKB1. *Oncogene.* 2018;37(23):3045–3057.
29. Momcilovic M, Shackelford DB. Targeting LKB1 in cancer – exposing and exploiting vulnerabilities. *Br J Cancer.* 2015;113(4):574–584.
30. Mihaylova MM, Shaw RJ. The AMPK signalling pathway coordinates cell growth, autophagy and metabolism. *Nat Cell Biol.* 2011;13(9):1016–1023.
31. Teague TT, Payne SR, Kelly BT, et al. Evaluation for clinical benefit of metformin in patients with idiopathic pulmonary fibrosis and type 2 diabetes mellitus: a national claims-based cohort analysis. *Respir Res.* 2022;23(1):91.
32. Han SH, Malaga-Dieguez L, Chinga F, et al. Deletion of Lkb1 in renal tubular epithelial cells leads to CKD by altering metabolism. *J Am Soc Nephrol.* 2016;27(2):439–453.
33. Bai T, Yang Y, Wu YL, et al. Thymoquinone alleviates thioacetamide-induced hepatic fibrosis and inflammation by activating LKB1-AMPK signaling pathway in mice. *Int Immunopharmacol.* 2014;19(2):351–357.
34. Lizcano JM, Göransson O, Toth R, et al. LKB1 is a master kinase that activates 13 kinases of the AMPK subfamily, including MARK/PAR-1. *EMBO J.* 2004;23(4):833–843.
35. Goodwin JM, Svensson RU, Lou HJ, Winslow MM, Turk BE, Shaw RJ. An AMPK-independent signaling pathway downstream of the LKB1 tumor suppressor controls Snail1 and metastatic potential. *Mol Cell.* 2014;55(3):436–450.
36. Roy BC, Kohno T, Iwakawa R, et al. Involvement of LKB1 in epithelial-mesenchymal transition (EMT) of human lung cancer cells. *Lung Cancer.* 2010;70(2):136–145.
37. Hill C, Wang Y. The importance of epithelial-mesenchymal transition and autophagy in cancer drug resistance. *Cancer Drug Resist.* 2020;3(1):38–47.
38. Hill C, Wang Y. Autophagy in pulmonary fibrosis: friend or foe? *Genes Dis.* 2022;9(6):1594–1607.
39. Gsurumrthy S, Xie SZ, Alagesan B, et al. The Lkb1 metabolic sensor maintains haematopoietic stem cell survival [published correction appears in *Nature*. 2011 Aug 4;476(7358):114]. *Nature.* 2010;468(7324):659–663.
40. Araya J, Nishimura SL. Fibrogenic reactions in lung disease. *Annu Rev Pathol Mech Dis.* 2010;5:77–98.
41. Sanchez-Garrido J, Shenoy AR. Regulation and repurposing of nutrient sensing and autophagy in innate immunity. *Autophagy.* 2021;17(7):1571–1591.